7722 *Biochemistry* **2010,** *49,* 7722–7732
DOI: 10.1021/bi100735v

BIOCHEMISTRY
including biophysical chemistry & molecular biology
Article

Lipid Bilayer-Assisted Release of an Enediyne Antibiotic from Neocarzinostatin Chromoprotein†

Parameswaran Hariharan,‡,§ Christopher Gunasekaran Sudhahar,‡ Shan-Ho Chou,§ and Der-Hang Chin*,‡

‡*Department of Chemistry, National Chung Hsing University, Taichung 40227, Taiwan, ROC, and* §*Institute of Biochemistry, National Chung Hsing University, Taichung 40227, Taiwan, ROC*

Received May 10, 2010; Revised Manuscript Received June 30, 2010

ABSTRACT: The nine-membered enediyne class has drawn extensive interest because of extremely high antitumor potency and intricate interactions with its carrier protein. While the drug-induced DNA cleavage reactions have been mostly elucidated, the critical release−transport process of the labile enediyne molecule in cellular environment remained obscure. Using neocarzinostatin chromoprotein as a model, we demonstrated a lipid bilayer-assisted release mechanism. The *in vitro* enediyne release rate under aqueous conditions was found to be too slow to account for its efficient DNA cleavage action. Via the presence of lipid bilayers, chaotropic agents, or organic solvents, we found the release was substantially enhanced. The increased rate was linearly dependent on the lipid bilayer concentration and the dielectric value of the binary organic solvent mixtures. While lipid bilayers provided a low surrounding dielectricity to assist in drug release, there were no major conformational changes in the apo and holo forms of the carrier protein. In addition, the lifespan of the released enediyne chromophore was markedly extended through partitioning of the chromophore in the hydrophobic bilayer phase, and the lipid bilayer-stabilized enediyne chromophore significantly enhanced DNA cleavage *in vitro*. Collectively, we depicted how a lipid bilayer membrane efficiently enhanced dissociation of the enediyne chromophore through a hydrophobic sensing release mechanism and then acted as a protector of the released enediyne molecule until its delivery to the target DNA. The proposed membrane-assisted antibiotic release−transport model might signify a new dimension to our understanding of the modus operandi of the antitumor enediyne drugs.

The release and transport of bioactive small molecules that are naturally bound to carrier proteins are interesting topics in exploring fundamental and applied biosciences. The recently discovered nine-membered enediyne antibiotic chromoproteins (*1*, *2*), which belong to one of the most potent antitumor categories, are particularly attractive. While the drug-induced DNA cleavage reactions have been mostly elucidated, the intricate mode of action in the release−transport process remained unclear, even though such a process could critically affect drug efficacy. Among the members of the enediyne family, the first member, neocarzinostatin (NCS)[1] (*3*), is a very useful role model for studying small molecule−protein interactions (*4*). The NCS chromoprotein complex must first release its very tightly bound enediyne chromophore (NCS-C) (*5*), which is otherwise highly labile in a naked form (*6*, *7*). In the cellular environment, how the antibiotic is released and securely transported to the target DNA without losing its activity must be an ingeniously designed and adaptively evolved process.

NCS, isolated from *Streptomyces carzinostaticus* (*3*), is a 1:1 noncovalent complex (holoNCS) of NCS-C (*8*) and a protective apoprotein (apoNCS) (Figure 1) (*7*). The unique architecture of the nine-membered bicyclo[7,3,0]dodecadiyne ring (Figure 1A) makes NCS-C highly labile (*7*). A thiol-activated rearrangement of the enediyne core generates an active radical species, which abstracts hydrogen and leads to DNA lesions (*7*, *9*). Crystallography and solution NMR studies revealed that both holoNCS and apoNCS share a similar protein structure (*10*, *11*). apoNCS is an all-β-sheet protein (11 kDa) folded into a β-sandwich with overall dimensions of ~20 Å × 25 Å × 40 Å (*10*, *12*). The chromophore is bound in a deep cavity and is tightly secured by the two loops on the exterior of the binding cleft (Figure 1B).

Scientific interest in NCS is overwhelming because of its therapeutic usage as a potent antitumor drug (*13*, *14*). apoNCS carries the potent enediyne antibiotic and possesses attractive features as a prototype for the development of versatile cargo-delivery vehicles. Its small size and strong tolerance of denaturants (*15*) are favorable for an ideal drug carrier. With an immunoglobulin-like topology and attractive ligand binding scaffold, apoNSC provides a structural framework for the development of new recognition sites and binding specificities for nonenediyne molecules through protein engineering (*4*, *16*, *17*). At this

†This work was supported by Grant NHRI-EX90-8807BL from National Health Research Institutes and Grants 95-2311-B-005-012-MY3 and 95-2113-M-005-007-MY3 from the National Science Council, Taiwan, Republic of China, to D.-H.C. This work was also supported in part by the Ministry of Education, Taiwan, Republic of China, under the ATU plan to National Chung Hsing University.

*To whom correspondence should be addressed: Department of Chemistry, National Chung Hsing University, 250 Kuo-Kuang Rd., Taichung 40227, Taiwan, Republic of China. Telephone: +886-4-22840411, ext. 304. Fax: +886-4-22862547. E-mail: chdhchin@dragon.nchu.edu.tw.

[1]Abbreviations: NCS, neocarzinostatin; NCS-C, neocarzinostatin chromophore; apoNCS, apoprotein component of neocarzinostatin; holoNCS, chromoprotein complex of neocarzinostatin; PC, L-α-phosphatidylcholine; PS, L-α-phosphatidylserine; PE, L-α-phosphatidylethanolamine; LUV, large unilamellar vesicle; TBS, Tris-HCl-buffered saline; GSH, glutathione; MPS, 3-mercapto-1-propanesulfonic acid; CD, circular dichroism; HPLC, high-performance liquid chromatography.

 Published on Web 07/27/2010

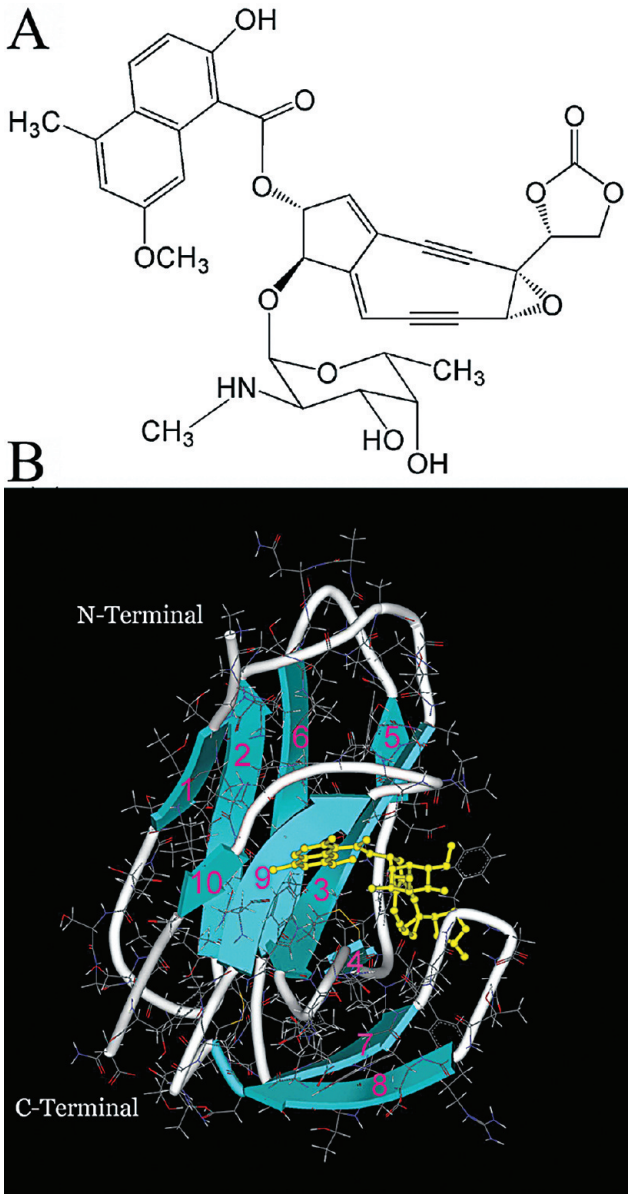

FIGURE 1: Structure of NCS-C (A) and holoNCS chromoprotein complex (B). The view of the aqueous holoNCS model at neutral pH was modified (*24*) from the Protein Data Bank crystal structure (entry 1nco).

juncture, given the potential scope of carrier apoNCS in therapeutic and biotechnological applications, identification of cellular events with respect to how its natural enediyne ligand is released has significant prospects.

We reported earlier that backbone conformational changes of apoNCS are not required for releasing NCS-C (*18*). Further mutational analysis revealed that a simple and specific side chain manipulation at Phe78 leads to efficient dissociation of NCS-C (*19*). Together, these studies imply some physiological factors underlying drug release. Because NCS-C binding has been suggested to be predominantly hydrophobic (*12*, *20*, *21*), here we focus on the low-dielectric effect of the lipid bilayer membrane on the release and protection of the drug. We provide crucial insights into the mode of release and transport *in vivo* and thereby manifest a plausible physiological mechanism for the antibiotic.

MATERIALS AND METHODS

Materials. NCS in powder form was a gift from Kayaku Co., Ltd. (Itabashi-Ku, Tokyo, Japan). A holoNCS stock solution of 0.5 mM (ε_{340} = 10800 M^{-1} cm^{-1}) was prepared and stored in aliquots in the dark at −80 °C. NCS-C was extracted from holoNCS (*22*) and stored in the dark at −80 °C in acidic methanol containing 20 mM sodium citrate (pH 4.0). The integrity and concentration of NCS-C were examined by HPLC analysis, and by UV spectrometry following titration of excess apoNCS. apoNCS was purified from the protein pellets (obtained from holoNCS after methanolic NCS-C extraction) using a Mono Q column of a FPLC system (AKTA purifier, GE Healthcare). Lipids L-α-phosphatidylcholine (PC) (from egg), L-α-phosphatidylserine (PS) (from bovine brain, Na salt), and L-α-phosphatidylethanolamine (PE) (from bovine liver) (Sigma Chemicals, St. Louis, MO) were dissolved and stored at 10 mg/mL in chloroform at −80 °C. Thiols used were of high-quality grade from Sigma-Aldrich (St. Louis, MO).

Preparation of Liposomes. Stock solutions of large unilamellar vesicles (LUVs) were prepared by a freeze−thaw and extrusion process in Tris-HCl-buffered saline (TBS) [25 mM Tris-HCl and 150 mM NaCl (pH 7.4)] (*23*). The freeze−thaw multilamellar lipid suspensions were extruded through double layers of a 100 nm nuclepore polycarbonate membrane (Whatman International Ltd.) at least 20 times using an Avanti Mini Extruder (Avanti Polar Lipids, Inc., Alabaster, AL) to generate uniformly sized LUVs. Negatively charged and neutral LUVs were prepared by combination of PC/PE/PS and PC/PE mixtures at molar ratios of 2:2:1 and 4:1, respectively. The phospholipid concentration of LUVs was determined by quantitative phosphorus analysis. The stock LUV solutions were stored at 4 °C and used within 7 days of preparation. Liposomes were prepared with a total lipid concentration of <5 mM regardless of the lipid composition and were freshly diluted to the desired concentration before being used.

Kinetics of Release of NCS-C from holoNCS. The rate of release of NCS-C from holoNCS was determined by an established fluorescence-based method (*18*, *19*). Negatively charged thiols, glutathione (GSH) and 3-mercapto-1-propanesulfonic acid (MPS), were used to trap the released NCS-C and convert it into a highly fluorescent adduct via the cycloaromatization reaction (*24*). For kinetic studies in the presence of LUVs, samples containing holoNCS (10 μM) in TBS saline (pH 7.4) without or with various concentrations of LUVs were prepared. After addition of 5 mM MPS, NCS-C release was monitored at 25 °C by following the increases in fluorescence emitted from the thiol−NCS-C adduct. The fluorescence intensity corresponding to 100% NCS-C release was determined by adding 2-propanol to a final concentration of 80% (v/v). Release kinetics in organic solvents and chaotropic salts were followed by fluorescence at 25 °C using samples containing 5 μM holoNCS, 100 mM Tris-HCl (pH 7.0), and 5 mM GSH with various concentrations of organic solvents or chaotropic salts. The rate constant was estimated from the initial 10% release (or 50% release in the case of kinetics in the presence of chaotropic salts) that fits into a first-order linear plot (ln[holoNCS] vs time). Release kinetics in LUVs were also independently followed by HPLC analyses of the progressive reaction of MPS with unbound NCS-C on aliquots (1.0 nmol) drawn from incubated holoNCS samples at different time points.

HPLC. A Waters (Milford, MA) Millennium HPLC system equipped with a model 600E solvent delivery system, a 996 photodiode array detector, and a either Waters 474 or Jasco (Tokyo, Japan) FP-1520 fluorescence detector was used as described previously (*25*). NCS samples (0.5−1 nmol) were

analyzed through a Waters μ-Bondapak reverse phase C18 column (particle size, 10 μm; pore size, 125 Å; 39 mm × 330 mm) using an established gradient (*25*). The remaining amounts of protein-bound NCS-C (intact form) and released NCS-C that had been converted into a thiol−NCS-C adduct were analyzed by integrating the corresponding chromatographic peak area monitored via UV absorbance (A_{226}) (*25*).

Chromophore Protection. To examine the chromophore protection efficiency of LUVs and to compare them with that of apoNCS, NCS-C (27 μM) was incubated in TBS (pH 7.4) for different time intervals in the presence of an equimolar amount of apoNCS or 2 mM LUVs in a total volume of 45 μL in the dark at 25 °C. The methanol content in each sample (introduced by NCS-C stock) was kept constant at 10% (v/v). Following by an incubation period of 10−180 min, excess apoNCS (1.25-fold excess) was added to stop further degradation of NCS-C. The remaining amount of NCS-C in each sample was analyzed by HPLC (*25*).

Fluorescence Spectroscopy. The rate of release of NCS-C from holoNCS in the presence of organic solvents was measured with a Hitachi (Tokyo, Japan) F4500 spectrofluorimeter using a method described previously (*18*). Fluorescence changes corresponding to NCS-C release kinetics in the presence of LUVs or chaotropic salts were monitored by a SLM Aminco Bowman Series II luminescence spectrometer (SLM Aminco Bowman). A thermostatic cell holder kept the sample (150 μL) temperature at 25 °C in a 3 mm square quartz cell. By excitation at 340 nm, single-point data for emission at 440 nm were acquired once every 30 s. To avoid NCS degradation by excessive exposure to the light source, the time scan mode was modified by a written macro language to enable closing of the light shutter between measurements. Fluorescence spectra were recorded with the same instrument at 25 °C from 5 μM NCS-C in respective solvents with or without apoNCS or LUVs. Emission spectra for all samples were recorded with excitation at 340 nm at a fixed detector voltage. Each spectrum was subtracted from the respective buffer blank recorded independently under the same conditions.

Circular Dichroism. All circular dichroism (CD) measurements were taken on a Jasco J-715 spectropolarimeter equipped with a circulating water bath (model RTE-140, Neslab, Portsmounth, NH). The instrument was calibrated with ammonium *d*-10-camphor sulfonate. To obtain CD spectra in LUVs, NCS samples were prepared in 200 μL of TBS (pH 7.4) with or without 1 mM LUVs. The concentrations of apoNCS used for far-UV CD, near-UV CD with LUVs, and near-UV CD without LUVs were 10, 40, and 53 μM, respectively. The concentration of the holoNCS sample, with or without LUVs, was 15 μM throughout. Each spectrum was recorded at 25 °C using a temperature-controlled water-jacketed cell with a path length of 0.1 cm. The scan speeds used for measuring apoNCS and holoNCS were 20 and 100 nm/min, respectively. The far-UV and near-UV CD spectra of apoNCS in organic solvents were recorded at 25 °C following the method described previously (*15*). apoNCS samples (10 μM) were prepared in a mixed buffer of 2.67 mM ammonium acetate and 20 mM sodium acetate (pH 5) containing a requisite percentage (v/v) of organic solvents. All spectra were recorded a minimum of five times and were corrected for the respective buffer blanks. The results were expressed as mean residue ellipticity, [θ], which is defined as $\theta_{obs}/(113lc)$, where θ_{obs} is the observed ellipticity in degrees, c is the concentration in decimoles per liter, l is the length of the light path in centimeters, and the constant 113 is the number of residues in apoNCS.

DNA Cleavage. The extent of DNA damage induced by NCS was evaluated by following the conversion of supercoiled pBR322 DNA (form I) into relaxed circular (form II) and linear duplex forms (form III). NCS-C samples (1 μM) prepared in TBS (pH 7.4) were preincubated with 1 mM PC/PE or PC/PE/PS LUVs in the dark at 25 °C for 60 min before the reaction with DNA. The preincubated NCS-C at a final concentration of 50 nM was mixed with 200 ng of pBR322 DNA, 5 mM GSH, 100 mM Tris-HCl (pH 7.1), and 2.5 mM EDTA in a total reaction volume of 20 μL. Samples were incubated at 25 °C for 60 min, followed by electrophoresis in a 1% (w/v) agarose gel at 100 V. The gel was stained with 0.5 mg/mL ethidium bromide and documented in a UV transilluminator with a fluorimager Alpha Imager 2000 (Alpha Innotech Corp., San Leandro, CA).

RESULTS

NCS-C Release Was Greatly Enhanced by LUVs. Previously, we designed a simulated and simplified equilibrium disturbing operation *in vitro* by monitoring the chromophore release in the presence of an excess thiol such as GSH or MPS that efficiently inactivates the released NCS-C (*18*, *19*). The mimicked mechanistic process we studied shows a fairly slow antibiotic release rate under aqueous and neutral conditions. Such a slow releasing process of NCS-C (0.18 to 0.19 h^{-1}) is incompatible with its very efficient DNA cleavage action in nature. To explore the release mechanism in the cellular environment, we investigated the possible role of membranes in assisting antibiotic release. To mimic biological membranes, purified liposomes of LUVs containing a mixture of naturally abundant phospholipids, PC, PE, and PS, were used in this study. The neutral and negatively charged LUVs were obtained by mixing PC and PE and by mixing PC, PE, and PS, respectively. The mean diameter of the LUVs was estimated to be 100 nm, which is approximately one-fifth million times larger than that of apoNCS.

A negatively charged thiol such as MPS or GSH is effectively shielded by acidic NCS protein but reacts quickly with the released NCS-C to form a highly fluorescent thiol−NCS-C adduct (*24*). This unique reaction has been utilized as an indicator to follow the release process of NCS-C (*18*, *19*). To investigate the effect of LUVs on the NCS-C release rate, aliquot samples of holoNCS containing excess MPS in the absence or presence of PC/PE or PC/PE/PS LUVs were incubated at pH 7.4 and subjected to HPLC analysis. Figure 2 shows chromatographic profiles monitored by both UV absorbance and fluorescent emission. All major peaks were further identified by UV spectroscopic and MS analyses (*25*). Peak **1** was characterized as the intact NCS-C (MH^+, m/z 660), corresponding to those remaining protein-bound NCS-C molecules. Peak **2** was the MPS−NCS-C adduct (m/z 818 and 840 for mono- and disodium salt, respectively), corresponding to the released NCS-C. Extended incubation resulted in the production of peak **3** at the expense of **2**. Both **2** and **3** shared similar UV spectroscopic characteristics (*25*), suggesting that degradation of **2** generated **3**. Quantitative analyses showed that, in the absence of LUVs, ~79 ± 3% of NCS-C remained protein-bound after incubation for 3 h at room temperature (Figure 2A), which was consistent with an earlier observation using GSH in 100 mM Tris-HCl (pH 7.0) (*19*). Strikingly, in the presence of LUVs (Figure 2B,C), none of the protein-bound NCS-C remained and all were released under the

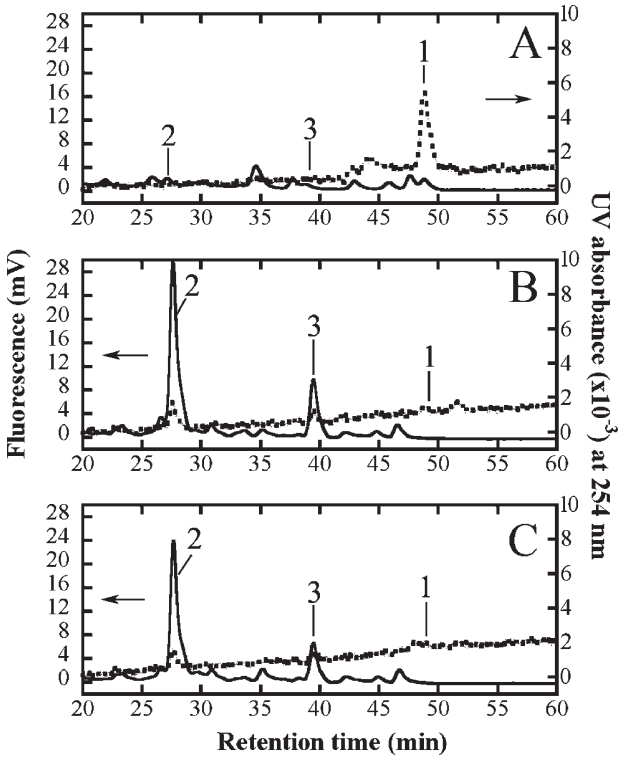

FIGURE 2: Effect of LUVs on NCS-C release analyzed by HPLC. HPLC chromatograms of UV absorbance at 254 nm (---) were overlaid with that of fluorescence emission at 440 nm (excitation at 340 nm) (—). holoNCS samples were incubated with 5 mM MPS in (A) TBS buffer alone, (B) PC/PE LUVs, or (C) PC/PE/PS LUVs. Peak **1** was characterized as the intact (protein-bound) NCS-C. **2** was the MPS-inactivated (released) NCS-C. **3** was the degraded product of **2**.

same conditions. The results provided a good indication that the biological membrane might effectively enhance the release of NCS-C from the holoNCS complex.

Release Kinetics in LUVs Followed by Fluorescence. Using the negatively charged thiol MPS as a release indicator, the kinetics of the LUV-assisted NCS-C release were studied by following the established fluorescence method (*18*, *19*). In the absence of LUVs, the decreased rate of holoNCS concentration caused by NCS-C release was slow (Figure 3A,B). However, a rapid decrease was observed in the presence of both types of LUVs, suggesting an accelerated NCS-C release. The effect of different types of LUVs on the rate of NCS-C release was found to be unequal. The neutral type PC/PE LUVs (Figure 3A) appeared to be more efficient in assisting the release than the negatively charged PC/PE/PS LUVs (Figure 3B). At the 1 mM level, the presence of PC/PE and PC/PE/PS LUVs resulted in ~90 and ~70% NCS-C release, respectively, after incubation for 60 min at room temperature. On the other hand, only 13% release was observed in the absence of LUVs.

Figure 3C shows HPLC quantitative analysis of the remaining amount of the protein-bound NCS-C after incubation for 30 min with different levels of LUVs. The results revealed a clear LUV concentration dependence of NCS-C release and corresponded well with that obtained from fluorescence measurements (Figure 3A). The rate constant k that fitted into a first-order linear plot was estimated by following the fluorescence changes with time using MPS as a release indicator (Table 1). For holoNCS samples in TBS (pH 7.4) alone, the release rate was $0.18 \pm 0.04\ h^{-1}$ at 25 °C, which was close to that obtained earlier using GSH at pH 7.0 ($0.19 \pm 0.01\ h^{-1}$) (*19*). In the presence of LUVs, the observed NCS-C release rate constants increased with an increase in lipid bilayer concentration. Drastic increases in the release rate of 37- and 19-fold were observed with 1 mM PC/PE and PC/PE/PS LUVs, respectively. The plots of the observed k values versus LUV concentration demonstrated a closely correlated linear dependence (correlation coefficient $R = 0.999$ and 0.977 for PC/PE and PC/PE/PS LUVs, respectively) (Figure 3D). The displayed slopes suggested efficiencies of ~6.5 and ~3.6 h^{-1}/mM PC/PE and PC/PE/PS LUVs, respectively, in increasing the NCS-C release rate. Collectively, the observed effect of the presence of LUVs on the release rate illuminated the possibility of the phospholipid bilayer being a major and effective factor in assisting in NCS-C release in a physiological environment.

Circular Dicroism-Based Structural Characterizations. The far-UV CD spectrum of native apoNCS shown in Figure 4A had a typical negative ellipticity at 212 nm for β-sheet secondary structure and a characteristic positive ellipticity at 224 nm. The near-UV CD of apoNCS (Figure 4A, inset), which corresponds to the tertiary structure, exhibited a weak negative ellipticity centered at 271 nm. Both far- and near-UV CD spectra of apoNCS were consistent with reports (*19*, *26*, *27*). Similar to apoNCS, holoNCS also exhibited an intense far-UV CD signal at 224 nm but showed an additional prominent negative signal around 255 nm that resulted from the protein-bound NCS-C (Figure 4B) (*28*, *29*). Unlike NCS, neither PC/PE nor PC/PE/PS LUVs up to 1 mM exhibited any intrinsic ellipticity signals between 200 and 400 nm (data not shown). This feature enabled us to reliably detect structural changes of NCS protein in the presence of LUVs through CD measurements. Close inspection of the CD spectra of apoNCS containing the LUVs (Figure 4A) revealed no significant changes in spectra in both far- and near-UV regions, indicating that both the secondary and tertiary structures of apoNCS were not disturbed by the presence of LUVs. Similar to apoNCS, holoNCS samples prepared in both types of LUVs did not significantly alter the characteristic CD pattern (Figure 4B). Collectively, the results of CD spectroscopy indicated an undisturbed protein backbone conformation of apoNCS and holoNCS by the presence of LUVs.

We also examined changes in the apoNCS CD spectrum in aqueous solutions containing various levels of hydrophobic organic solvents. The far-UV CD spectrum of apoNCS (Figure 4C, left column) remained unchanged until 70% (v/v) methanol, 65% (v/v) ethanol, 65% (v/v) 2-propanol, and 80% (v/v) acetonitrile, indicating the high endurance of the secondary structure of apoNCS. The tertiary structure of apoNCS monitored by near-UV CD spectra (Figure 4C, right column) showed disruption only beyond 65% (v/v) methanol, 60% (v/v) ethanol, 60% (v/v) 2-propanol, and 60% (v/v) acetonitrile.

NCS-C Release Was Enhanced under Low-Dielectric Conditions. By employing the organic solvents that cover a wide range of dielectricity, we explored whether hydrophobicity was involved in the NCS-C release mechanism. Because protein denaturation facilitated ligand release, to avoid complications, we followed the release kinetics by introducing various amounts of organic solvents at concentrations at which the apoNCS conformation remained unchanged. Using excess GSH at pH 7 as a release indicator, the observed release rates estimated by fluorescence changes were found to increase notably at a concentration of the organic solvent beyond the inflection point (approximately 15−35%, depending upon the types of organic solvents) (Figure 5A). At 30% 2-propanol, 40% ethanol, 53%

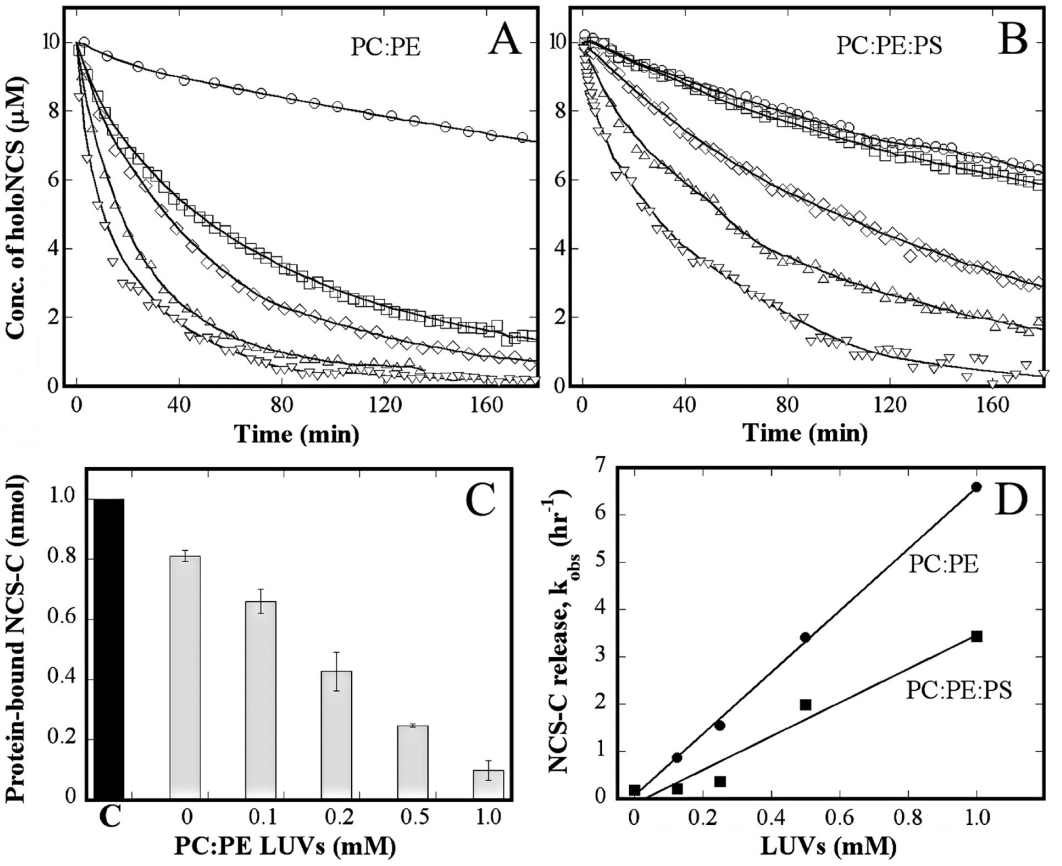

FIGURE 3: Effect of LUVs on the kinetics of NCS-C release. Panels (A) and (B) show temporal release of NCS-C from 10 μM holoNCS monitored by fluorescence using 5 mM MPS as a release indicator. Changes in the concentration of holoNCS with time were monitored at 25 °C in TBS buffer alone (○) or in the presence of (A) PC/PE or (B) PC/PE/PS LUVs at a concentration 0.125 (□), 0.25 (◇), 0.5 (△), and 1 mM (▽). (C) HPLC quantitative analysis of the remaining protein-bound NCS-C after incubation with PC/PE LUVs at 25 °C for 30 min. Column C denotes the control (holoNCS sample in TBS buffer alone without MPS or LUVs). (D) Observed rate constants of NCS-C release at various concentrations of PC/PE (●) and PC/PE/PS (■) LUVs.

Table 1: Observed Kinetic Rates of NCS-C Release at Different Levels of LUVs

sample	k_{obs} (h^{-1}) of NCS-C release at 25 °C[a]	increase in release rate (*x*-fold)
natural holoNCS[b]	0.18 ± 0.04 (5)	–
with PC/PE LUVs		
0.125 mM	0.86 ± 0.07 (5)	4.8
0.25 mM	1.55 ± 0.07 (6)	8.6
0.5 mM	3.40 ± 0.15 (5)	18.9
1 mM	6.59 ± 0.38 (3)	36.6
with PC/PE/PS LUVs		
0.125 mM	0.21 ± 0.03 (3)	1.2
0.25 mM	0.36 ± 0.03 (3)	2.0
0.5 mM	1.98 ± 0.11 (3)	11.0
1 mM	3.43 ± 0.19 (3)	19.1

[a]The k_{obs} value was estimated from the initial 10% release rate. The number in parentheses stands for the number of repetitions, from which the data were averaged. [b]For 10 μM holoNCS samples in TBS (pH 7.4) containing 5 mM MPS.

methanol, and 55% acetonitrile, the release rate increased to a level of 50 h^{-1} (approximately half of the maximum release rate prior to protein denaturation) (Figure 5A).

Figure 5A revealed that the relative efficiencies in assisting NCS-C release measured at 25 °C were in the following order: 2-propanol > ethanol > methanol ≈ acetonitrile. This was consistent with the order of the magnitudes of dielectric constant obtained at 25 °C: 2-propanol (19.264) > ethanol (24.852) > methanol (32.613) ≈ acetonitrile (35.688) (*30*). To adequately evaluate the surrounding hydrophobicity for the drug, we estimated the relative dielectricity (ε_r) of the solvent mixtures by adopting a linear dependence of the dielectric constants observed in the binary systems (*31*). A plot of the observed NCS-C release rate constant k versus the solvent ε_r value showed a pronounced increase in release rate at ε_r values of <70 F/m (Figure 5B). Interestingly, the release rates not only increased linearly with decreased ε_r values but also merged together somewhat irrespective of the type of organic solvent. At the NCS-C release rate of 50 h^{-1}, the ε_r value of the solution was constrained within 57 ± 3 F/m, indicating environmental dielectricity to be a major factor influencing drug release.

Hydrophobicity Was Involved in the NCS-C Release Mechanism. Chaotropic salts in the Hofmeister series such as $NaClO_4$ have been successfully employed to demonstrate hydrophobic interaction of the enediyne antibiotic calicheamicin with DNA (*32*). By adding perchlorate salts, we found that the NCS-C release rate increased linearly with an increase in the salt concentration (Figure 5C), demonstrating that the association of NCS-C with apoNCS was hydrophobic in nature. By hydrophobic perturbation, the weakly hydrated $NaClO_4$ enhanced the NCS-C release at an efficiency of 0.025 h^{-1} per molar concentration of the salt. A similar but more obvious hydrophobic perturbation effect in 15% ethanol was observed using NH_4ClO_4

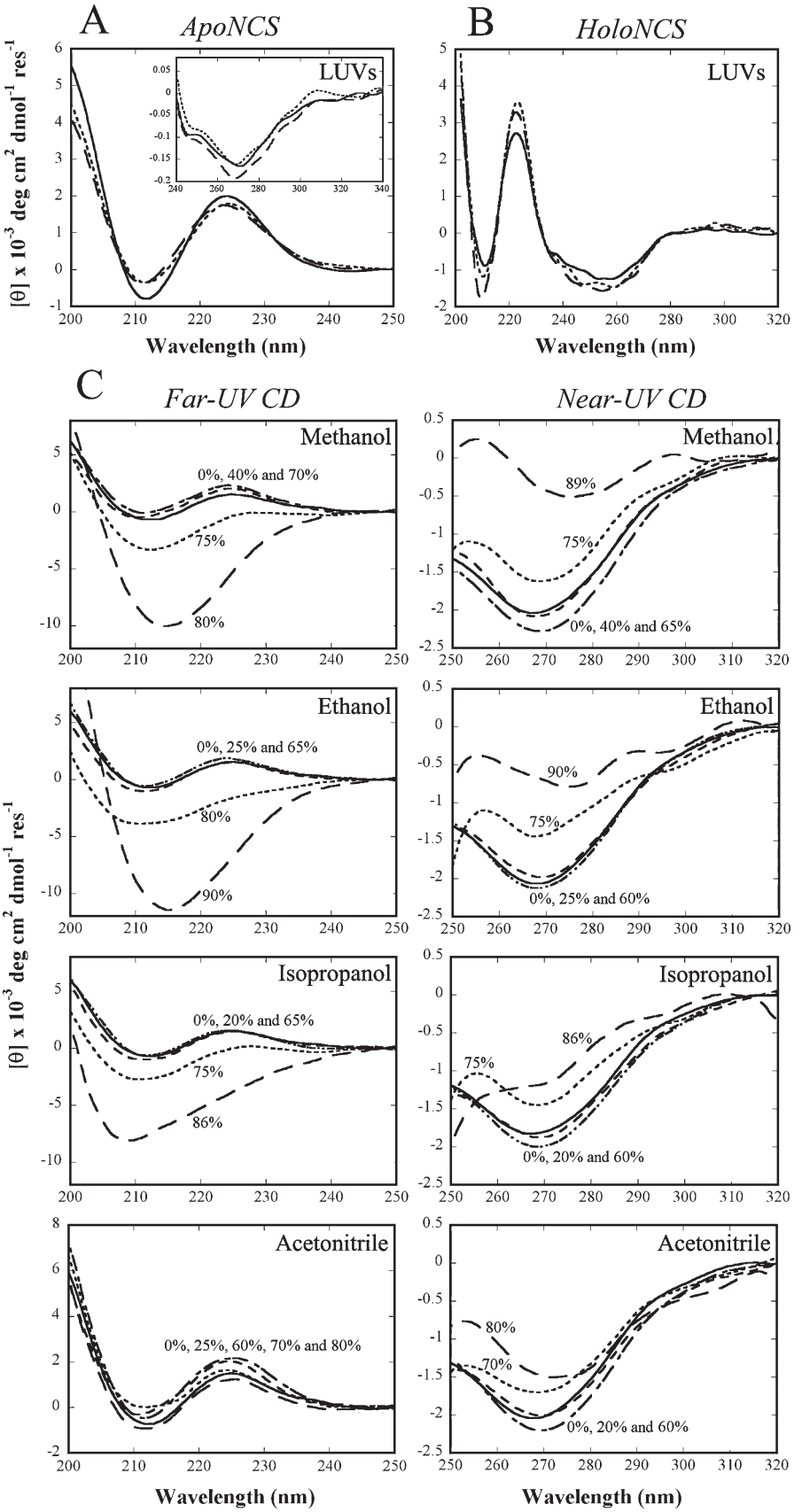

FIGURE 4: CD spectra of NCS in the presence of LUVs and organic solvents. (A) Far-UV and near-UV (inset) CD spectra of apoNCS with or without LUVs. (B) CD spectra of holoNCS with or without LUVs. The CD spectra were recorded at 25 °C in the presence of 1 mM PC/PE (---) or 1 mM PC/PE/PS (− − −) LUVs or only TBS (pH 7.4) (—). (C) Far-UV (left column) and near-UV (right column) CD spectra of apoNCS in the presence of respective organic solvents. All results are expressed as mean residue ellipticity, [θ].

to perturb the nonpolar interaction between NCS-C and apoNCS (Figure 5C, inset). [Note that chaotropic agents like $NaClO_4$ tend to destabilize proteins (*33*). We found that apoNCS began to denature beyond 5 M $NaClO_4$, in which the efficiency

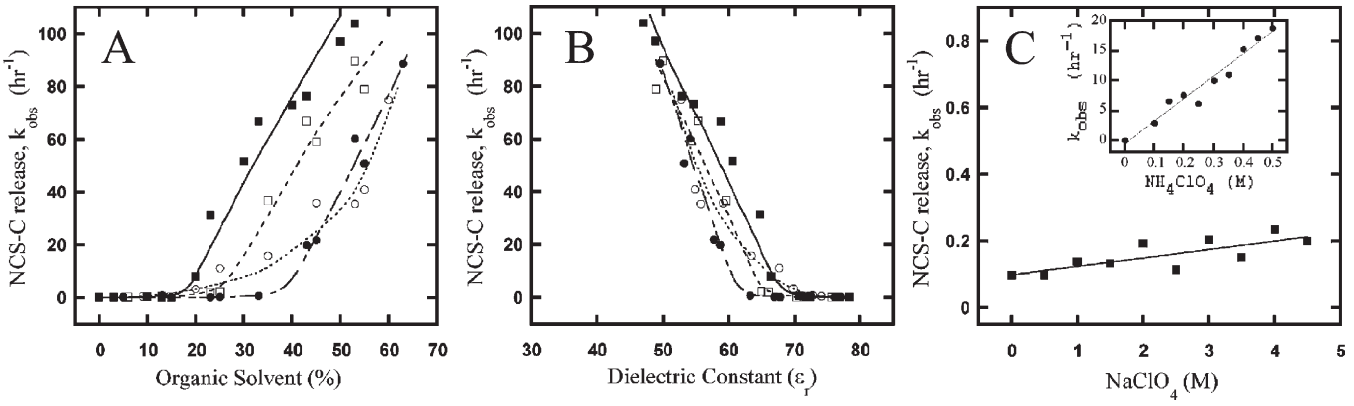

FIGURE 5: Kinetics of NCS-C release in the presence of organic solvents and salts. (A) Kinetic rates of NCS-C release in aqueous solutions containing organic solvents at various concentration levels (%, v/v): 2-propanol (■, —), ethanol (□, ---), methanol (●, − − −), and acetonitrile (○, · · ·). (B) Observed rate constants of NCS-C release against respective dielectricity (ε_r) of organic solvent/H_2O binary mixtures: 2-propanol (■, —), ethanol (□, ---), methanol (●, − − −), and acetonitrile (○, · · ·). (C) Observed rate constants of NCS-C release at different concentrations of chaotropic salts: $NaClO_4$ (■) and NH_4ClO_4 containing 15% ethanol (●) (inset). Kinetics of NCS-C release were monitored by fluorescence changes at 25 °C using GSH as a release indicator.

of inducing NCS-C release markedly increased from 0.025 to 9.7 h^{-1} per additional molar concentration of the salt. Such a large increase in release rate mainly resulted from protein denaturation and was beyond the scope of this study.]

The Released Enediyne Chromophore Was Stabilized by LUVs. To infer the drug mode in the cellular environment, we investigated the survival rate of the unbound NCS-C in lipid bilayers by quantitative analysis. As reversed phase HPLC has been proven to be a valuable tool for quick and efficient disruption of lipid bilayers (*34*), the remaining amount of NCS-C after incubation with LUVs at various time intervals could be determined reliably without interference. The analyses showed that the survival rate of NCS-C in LUVs was highly improved as compared to that in TBS alone (Table 2), suggesting that the lipid bilayers markedly extended the lifespan of the naked NCS-C. While the PC/PE type of LUV was more effective than the PC/PE/PS type in assisting drug release (Figure 3 and Table 1), it was also more effective in protecting the released NCS-C (Table 2).

NCS-C Partitioned in a Hydrophobic Lipid Environment. Because the neutral LUVs offered better protection of NCS-C than the negatively charged ones (Table 2), it is reasonable to assume hydrophobic partitioning to be a key factor in influencing the NCS-C survival rate. Fluorescence spectroscopy is sensitive to changes in environmental hydrophobicity and is often used to study molecular interactions between fluorescent drugs and lipids (*35*). To probe the phase in which the released NCS-C partitioned, fluorescence spectroscopy of NCS-C in aqueous solution was examined with or without LUVs and was compared with that in methanol. When NCS-C was excited at 340 nm, the fluorescence emission under aqueous conditions at pH 4 was centered at 441 nm (Figure 6A), which was close to the reported maximum value of 440 nm (*36*). When NCS-C was bound to the hydrophobic cavity of apoNCS, the spectrum had a blue shift with a fluorescence emission maximum at 433 nm (Figure 6A). The fluorescence emission spectra of NCS-C exhibited considerably large blue shifts (>30 nm) in aqueous solutions containing only 1 mM PC/PE or PC/PE/PS LUVs (Figure 6A), suggesting a strong partitioning into the hydrophobic phase of lipid bilayers. The very large blue shift by both types of LUVs signified that NCS-C preferred a hydrophobic lipid environment versus the hydrophilic aqueous phase. Note that the blue shift that resulted from methanol solvent (24.9 M) was comparable to that from LUVs at a level of only 1 mM (Figure 6A).

DNA Cleavage Induced by NCS-C in the Presence of LUVs. To examine whether the lipid-partitioned NCS-C could be efficiently utilized for DNA damage, NCS-C was preincubated with LUVs and subjected to a DNA cleavage reaction followed by agarose gel electrophoresis. The cleavage of the pBR322 plasmid was evidenced by conversion of the supercoiled form I (bottom band) into relaxed circular form II (top band) and linear duplex form III (middle band) (Figure 6B). Compared to the drug reaction without LUVs (lane 2), the NCS-C-induced DNA cleavage was markedly enhanced in samples incubated with PC/PE (lane 3) and PC/PE/PS (lane 4) LUVs. No cleavage of the plasmid was detected in the absence of NCS-C (lane 1) or in the presence of only LUVs (lanes 5 and 6).

DISCUSSION

The antitumor antibiotic NCS-C is produced *in vivo* along with its carrier protein. From an antibiotic perspective, NCS protein neither interacts with nor damages DNA (*5*, *37*). Only the released NCS-C intercalates with DNA and causes radical-based damage (*7*, *9*). The potent cytotoxicity of NCS thus critically depends on the efficient dissociation of NCS-C. The release of NCS-C from the chromoprotein complex and its DNA cleaving activity disturb the equilibrium between apoNCS and holoNCS by a constant dissociation and inactivation of NCS-C (*5*). However, the release of NCS-C from purified holoNCS *in vitro* is incompatibly slow, even under permissive physiological conditions (*5*, *18*, *19*, *38*). The availability of NCS-C conceivably relies on an external force to overcome its very high affinity for apoNCS ($K_d \leq 10^{-10}$ M) (*36*). To examine the release−transport process *in vivo*, and to locate potential cellular stimulants, we investigated the physiological role of membranes in assisting in the release of the antibiotic.

Low-Dielectric Conditions Caused NCS-C Release. The quantitative and kinetic studies in the presence of PC/PE and PC/PE/PS LUVs (Figures 2 and 3 and Table 1) revealed that NCS-C release prevailed in the vicinity of lipid bilayers and the increased rate was dependent on lipid concentration. The more hydrophobic PC/PE vesicles (neutral in charge) had a higher efficiency

Table 2: Percentages of NCS-C Remaining after Incubation with LUVs

incubation time at 25 °C (min)	in TBS[a] alone	with equimolar apoNCS in TBS	in 2 mM PC/PE LUVs in TBS	in 2 mM PC/PE/PS LUVs in TBS
10	0 (not detected)	97 ± 6	82 ± 3	69 ± 5
60	0 (not detected)	88 ± 2	65 ± 3	45 ± 2
180	0 (not detected)	83 ± 2	35 ± 2	32 ± 1

[a]All samples of NCS-C (27 μM) were incubated in TBS buffer (pH 7.4) without a thiol at 25 °C in the dark. The methanol content for each sample was kept constant at 10% (v/v). Degradation of NCS-C was not detectable in a solution containing a 1.2-fold excess of apoNCS, and the analyzed NCS-C amount was taken to be 100%.

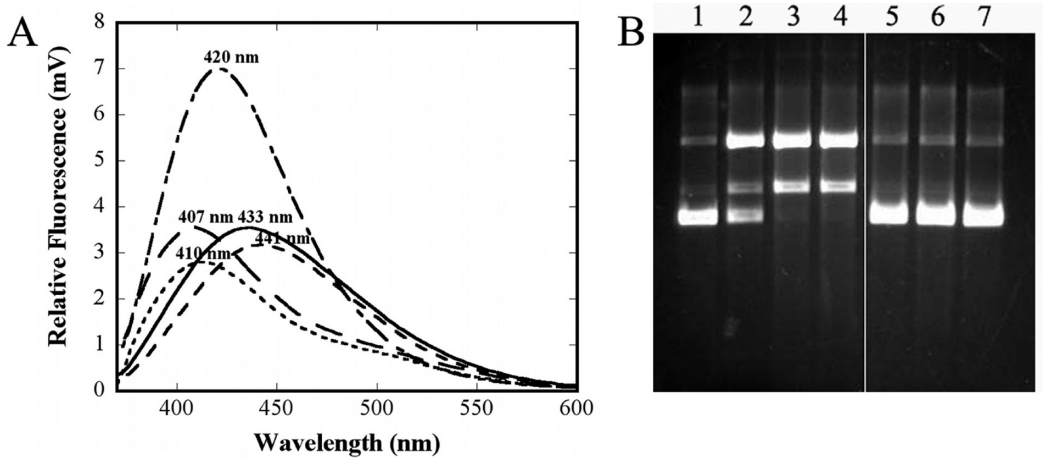

FIGURE 6: Effect of LUVs on the NCS-C fluorescence spectra and its DNA cleavage activity. (A) Fluorescence spectra of NCS-C (5 μM) in (i) methanol containing 0.1 M ammonium acetate (pH 4.0) (- — -), (ii) an aqueous solution containing 25 mM sodium citrate (pH 4.0) in the absence (− − −) or presence (—) of 1:1 apoNCS, and (iii) an aqueous solution containing 1 mM PC/PE/PS (— — —) or PC/PE (-----) LUVs in TBS buffer (pH 7.4). (B) NCS-C-mediated DNA cleavage in the presence of LUVs was analyzed by agarose gel (1%, w/v) electrophoresis. The reaction samples containing 200 ng of pBR322 were incubated for 1 h in the absence (lane 1) or presence of the preincubated NCS-C (50 nM) in only TBS (pH 7.4) (lane 2) or TBS with 1 mM PC/PE (lane 3) or PC/PE/PS LUVs (lane 4). Controlled reaction mixtures lacking NCS-C were assessed in TBS (pH 7.4) containing 1 mM PC/PE (lane 5) or 1 mM PC/PE/PS LUVs (lane 6) or without LUVs (lane 7).

in stimulating release than the less hydrophobic PC/PE/PS (negatively charged) LUVs (see Figures 2 and 3 and Table 1).

The kinetic study of NCS-C release in organic solvents (Figure 5A) and chaotropic salts (Figure 5C) revealed hydrophobicity to be an important factor involved in the release mechanism under a condition when the protein was not unfolded. Dissociation of NCS-C was mainly a consequence of disturbing the hydrophobic interaction between NCS-C and apoNCS and thus was dependent on the environmental dielectric value (Figure 5B). While protein denaturation facilitates rapid drug release, the hydrophobicity-dependent release without protein denaturation could be a controllable way to regulate the availability of the drug. Correspondingly, the lipid bilayers, which efficiently enhanced NCS-C release, have a very low dielectricity at the bilayer interface between the two alkyl chains (~2 F/m), and a considerably low value at the polar head region (25−40 F/m) (*39*, *40*). Overall, our results corroborated that the release of enediyne from NCS chromoprotein mainly occurred through hydrophobic perturbations caused by the low-dielecricity effect of lipid bilayers.

A recent NMR structure and dynamics investigation (*11*) suggests the existence of more than one equilibrium state for holoNCS, i.e., a "closed or strong binding state" under stabilizing aqueous conditions and an "open or weak binding state" under hydrophobic or other permissible conditions. The study described above implies that dynamics and internal motions of the binding cleft are likely to play key roles in the ligand release process. Fluorescence anisotropy studies and molecular dynamics simulations suggest that proteins in organic solvents with low dielectricity often reduce overall structural flexibility (*41*, *42*). Accordingly, the release of NCS-C in a solution containing the low-dielectric lipid bilayers might be enhanced by a reduction in the flexibility of holoNCS in the ligand binding region. NMR relaxation studies under aqueous conditions suggest that backbone of holoNCS is more flexible than that of apoNCS (*43*). Such a phenomenon is not rare in proteins with hydrophobic ligand binding (*44*). Flexibility reduction in holoNCS under low-dielectric conditions might shift the protein into a permissible open or weak binding state, which subsequently aids the diffusion of the ligand into the outer solvent.

Hydrophobic Sensing Release of NCS-C Did Not Require Major Protein Structural Changes. Given the versatility of bioactive molecule−protein interaction networks (*45*), such as immune systems (*46*), enzyme complexes (*47*), and many protein−ligand complexes (*48*), a mechanism resembling a lock and key is still prevalent. Dissociation of a high-affinity ligand from carrier proteins often requires protein backbone conformational changes that can be triggered by some cellular effectors (*45*). On the other hand, some proteins exhibit the smallest differences in the protein architecture upon ligand release. Proteins that bind to retinols, pheromones, or fatty acids are a few examples (*49*−*51*). The ligand association generally involves only a minimal "induced fit", in which typically a noncovalent interaction occurs on preassembled binding cleft of the protein with only minor side chain movements (*47*).

The CD-based structural characterization of the apo and holo forms in the presence of lipid bilayers revealed a preserved native

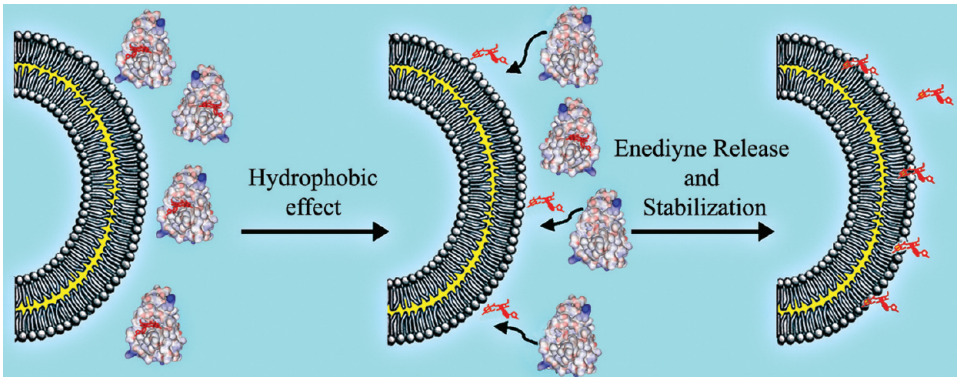

FIGURE 7: Model for lipid membrane-assisted drug release.

conformation (Figure 4A,B). Similar studies in organic solvents (Figure 4C) further confirmed that the NCS-C release preceded major secondary and tertiary structural changes of apoNCS (Figure 5A). Our hypothesis of NCS-C release in LUVs was that NCS experienced a local environmental hydrophobic perturbation rather than direct structural alterations of the protein. This hydrophobic sensing release mechanism could well happen without major structural changes of the protein. An *in vitro* study of cellular retinol binding protein type 1 shows a similar tendency to dissociate the hydrophobic ligand in water/alcohol mixtures under low-dielectric conditions without protein denaturation (*52*). The ligand release mechanism that we proposed here might represent a common pathway for hydrophobic ligand release in a situation where the bound and unbound protein conformations share a similar structure.

The Released Enediyne Chromophore Was Stabilized by LUVs. Without binding with macromolecules such as apoNCS or DNA, the naked NCS-C faces immediate threats of chemical inactivation and degradation in the aqueous milieu, which is unfavorable for drug delivery (*6*, *7*, *9*, *36*, *53*). The natural carrier apoNCS has been reported to be the best stabilizer among all other known agents such as DNA, albumin, organic solvents, etc. (*6*, *36*). Although not as effective as that of apoNCS, the protecting efficiency of 2 mM PC/PE LUVs was quite remarkable and nearly comparable to that of 1:1 apoNCS within a 10 min time interval (Table 2). Considering that a 10 min incubation of NCS with cells is sufficient to cause extensive DNA damage (*6*), the very high concentration of phospholipids in the cellular membrane environment should provide sufficient protection to the released enediyne chromophore until it reaches the target DNA *in vivo*. Fluorescence studies suggested that the released NCS-C partitioned in a hydrophobic lipid phase of LUVs (Figure 6A). Partitioning of a nonpolar molecule across the hydrophobic core region of the membrane has been observed for many compounds and is not an uncommon phenomenon (*54*, *55*). Because of the labile nature of NCS-C, it is beyond the scope of this investigation to conduct elaborate binding studies to establish the molecular details of the interaction between the LUVs and NCS-C. However, the potential of the lipid-partitioned NCS-C to cleave the plasmid DNA signified the role of lipid bilayers in preserving NCS-C activity (Figure 6B). Partitioning of NCS-C in the cellular membrane might be a chief mode of enediyne stabilization. In light of the high mobility in the cellular environment, the lipid bilayers could be considered as an ideal vehicle for *in vivo* drug transport.

Proposed Model for NCS-C Release and Transport Involving the Cellular Membrane. Release of NCS-C from holoNCS is the first key step of drug action (*5*). Although internalization of NCS protein into eukaryotic cells has been observed (*56*, *57*), it remains unclear when and where the release occurs *in vivo*. This scenario showcased the conserved drug carrier function by lipid bilayers. The hydrophobicity as well as elasticity of the lipid bilayers could be specifically favorable for the release, stabilization, and even transportation of the labile enediyne molecules. The bioactive NCS-C molecules could journey through tripartite partners operating in the following order: from apoNCS to the membrane lipid bilayers and then the nucleus to exert its biological action on the target DNA (Figure 7). In the context described above, it is yet to demonstrate the spatiotemporal roles of the lipid bilayers after internalization of NCS in the cell. Nevertheless, these *in vitro* findings laid sufficient background and could open up new avenues for further studies in this line of research. Potentially, this lipid bilayer paradigm might be applicable across the whole enediyne family, including both the chromoprotein and nonchromoprotein types of members, as all of them share certain similarities in structure and properties (*58*). If the scenario governs the events accounting for the enediyne drug activity *in vivo*, its implications and deriving pharmaceutical benefits hold great promise.

ACKNOWLEDGMENT

We thank the Kayaku Co., Ltd., for the supply of NCS powder and Ms. Chiy-Mey Huang for assistance in HPLC analysis.

REFERENCES

1. Van Lanen, S. G., and Shen, B. (2008) Biosynthesis of enediyne antitumor antibiotics. *Curr. Top. Med. Chem. 8*, 448–459.
2. Jones, G. B., Lin, Y., Ma, D., Xiao, Z., Hwang, G. S., Kappen, L., and Goldberg, I. H. (2008) Congeners of the enediyne neocarzinostatin chromophore: Designed agents for bulged nucleic acid targets. *Curr. Top. Med. Chem. 8*, 436–447.
3. Ishida, N., Miyazaki, K., Kumagai, K., and Rikimaru, M. (1965) Neocarzinostatin, an antitumor antibiotic of high molecular weight. Isolation, physicochemical properties and biological activities. *J. Antibiot., Ser. A 18*, 68–76.
4. Baker, J. R., Woolfson, D. N., Muskett, F. W., Stoneman, R. G., Urbaniak, M. D., and Caddick, S. (2007) Protein-small molecule interactions in neocarzinostatin, the prototypical enediyne chromoprotein antibiotic. *ChemBioChem 8*, 704–717.
5. Jung, G., and Kohnlein, W. (1981) Neocarzinostatin: Controlled release of chromophore and its interaction with DNA. *Biochem. Biophys. Res. Commun. 98*, 176–183.
6. Kappen, L. S., and Goldberg, I. H. (1980) Stabilization of neocarzinostatin nonprotein chromophore activity by interaction with apoprotein and with HeLa cells. *Biochemistry 19*, 4786–4790.
7. Goldberg, I. H. (1991) Mechanism of neocarzinostatin action: Role of DNA microstructure in determination of chemistry of bistranded oxidative damage. *Acc. Chem. Res. 24*, 191–198.

8. Edo, K., Mizugaki, M., Koide, Y., Seto, H., Furihata, K., Otake, N., and Ishida, N. (1985) The structure of neocarzinostatin chromophore possessing a novel bicyclo[7,3,0]dodecadiyne system. *Tetrahedron Lett. 26*, 331–334.
9. Xi, Z., and Goldberg, I. H. (1999) DNA-damaging enediyne compounds. In Comprehensive Natural Products Chemistry (Barton, D. S., and Nakanishi, K., Eds.) pp 553−592, Elsevier, New York.
10. Kim, K. H., Kwon, B. M., Myers, A. G., and Rees, D. C. (1993) Crystal structure of neocarzinostatin, an antitumor protein-chromophore complex. *Science 262*, 1042–1046.
11. Takashima, H., Yoshida, T., Ishino, T., Hasuda, K., Ohkubo, T., and Kobayashi, Y. (2005) Solution NMR structure investigation for releasing mechanism of neocarzinostatin chromophore from the holoprotein. *J. Biol. Chem. 280*, 11340–11346.
12. Teplyakov, A., Obmolova, G., Wilson, K., and Kuromizu, K. (1993) Crystal structure of apo-neocarzinostatin at 0.15-nm resolution. *Eur. J. Biochem. 213*, 737–741.
13. Maeda, H., Edo, K., and Ishida, N., Eds. (1997) Neocarzinostatin: The past, present, and future of an anticancer drug, Springer-Verlag, Tokyo.
14. Abe, S., and Otsuki, M. (2002) Styrene maleic acid neocarzinostatin treatment for hepatocellular carcinoma. *Curr. Med. Chem.: Anti-Cancer Agents 2*, 715–726.
15. Sudhahar, C. G., and Chin, D.-H. (2006) Aponeocarzinostatin: A superior drug carrier exhibiting unusually high endurance against denaturants. *Bioorg. Med. Chem. 14*, 3543–3552.
16. Nicaise, M., Valerio-Lepiniec, M., Minard, P., and Desmadril, M. (2004) Affinity transfer by CDR grafting on a nonimmunoglobulin scaffold. *Protein Sci. 13*, 1882–1891.
17. Heyd, B., Pecorari, F., Collinet, B., Adjadj, E., Desmadril, M., and Minard, P. (2003) *In vitro* evolution of the binding specificity of neocarzinostatin, an enediyne-binding chromoprotein. *Biochemistry 42*, 5674–5683.
18. Sudhahar, G. C., Balamurugan, K., and Chin, D.-H. (2000) Release of the neocarzinostatin chromophore from the holoprotein does not require major conformational change of the tertiary and secondary structures induced by trifluoroethanol. *J. Biol. Chem. 275*, 39900–39906.
19. Hariharan, P., Liang, W., Chou, S.-H., and Chin, D.-H. (2006) A new model for ligand release. Role of side chain in gating the enediyne antibiotic. *J. Biol. Chem. 281*, 16025–16033.
20. Tanaka, T., Hirama, M., Ueno, M., Imajo, S., Ishiguro, M., Mizugaki, M., Edo, K., and Komatsu, H. (1991) Proton NMR Studies on the Chromophore Binding Structure in Neocarzinostatin Complex. *Tetrahedron Lett. 32*, 3175–3178.
21. Takahashi, K., Tanaka, T., Suzuki, T., and Hirama, M. (1994) Synthesis and binding of simple neocarzinostatin chromophore analogs to the apoprotein. *Tetrahedron 50*, 1327–1340.
22. Kuo, H.-M., Lee Chao, P.-D., and Chin, D.-H. (2002) Delocalized electronic structure of the thiol sulfur substantially prevents nucleic acid damage induced by neocarzinostatin. *Biochemistry 41*, 897–905.
23. Mayer, L. D., Hope, M. J., and Cullis, P. R. (1986) Vesicles of variable sizes produced by a rapid extrusion procedure. *Biochim. Biophys. Acta 858*, 161–168.
24. Chin, D.-H. (1999) Rejection by neocarzinostatin protein through charges rather than sizes. *Chem.—Eur. J. 5*, 1084–1090.
25. Chin, D.-H., Tseng, M.-C., Chuang, T.-C., and Hong, M.-C. (1997) Chromatographic and spectroscopic assignment of thiol induced cycloaromatizations of enediyne in neocarzinostatin. *Biochim. Biophys. Acta 1336*, 43–50.
26. Jayachithra, K., Kumar, T. K. S., Lu, T.-J., Yu, C., and Chin, D.-H. (2005) Cold instability of aponeocarzinostatin and its stabilization by labile chromophore. *Biophys. J. 88*, 4252–4261.
27. Heyd, B., Lerat, G., Adjadj, E., Minard, P., and Desmadril, M. (2000) Reinvestigation of the proteolytic activity of neocarzinostatin. *J. Bacteriol. 182*, 1812–1818.
28. Napier, M. A., Holmquist, B., Strydom, D. J., and Goldberg, I. H. (1981) Neocarzinostatin chromophore: Purification of the major active form and characterization of its spectral and biological properties. *Biochemistry 20*, 5602–5208.
29. Kandaswamy, J., Hariharan, P., Kumar, T. K., Yu, C., Lu, T. J., and Chin, D.-H. (2008) Is association of labile enediyne chromophore a mutually assured protection for carrier protein? *Anal. Biochem. 381*, 18–26.
30. Lide, D. R., Ed. (2005−2006) CRC Handbook of Chemistry and Physics, 86th ed., CRC Press, Boca Raton, FL.
31. Wagner, M., Stanga, O., and Schroer, W. (2003) Corresponding states analysis of the critical points in binary solutions of room temperature ionic liquids. *Phys. Chem. Chem. Phys. 5*, 3943–3950.
32. Ding, W. D., and Ellestad, G. A. (1991) Evidence for hydrophobic interaction between calicheamicin and DNA. *J. Am. Chem. Soc. 113*, 6617–6620.
33. Collins, K. D., and Washabaugh, M. W. (1985) The Hofmeister effect and the behavior of water at interfaces. *Q. Rev. Biophys. 18*, 323–422.
34. Wimley, W. C., and White, S. H. (1993) Quantitation of electrostatic and hydrophobic membrane interactions by equilibrium dialysis and reverse-phase HPLC. *Anal. Biochem. 213*, 213–217.
35. Zhang, J. Z., Hadlock, T., Gent, A., and Strichartz, G. R. (2007) Tetracaine-membrane interactions: Effects of lipid composition and phase on drug partitioning, location, and ionization. *Biophys. J. 92*, 3988–4001.
36. Povirk, L. F., and Goldberg, I. H. (1980) Binding of the nonprotein chromophore of neocarzinostatin to deoxyribonucleic acid. *Biochemistry 19*, 4773–4780.
37. Kappen, L. S., Napier, M. A., and Goldberg, I. H. (1980) Roles of chromophore and apo-protein in neocarzinostatin action. *Proc. Natl. Acad. Sci. U.S.A. 77*, 1970–1974.
38. Edo, K., Saito, K., Akiyama-Murai, Y., Mizugaki, M., Koide, Y., and Ishida, N. (1988) An antitumor polypeptide antibiotic neocarzinostatin: The mode of apo-protein−chromophore interaction. *J. Antibiot. 41*, 554–562.
39. Ashcroft, R. G., Coster, H. G., and Smith, J. R. (1981) The molecular organisation of bimolecular lipid membranes. The dielectric structure of the hydrophilic/hydrophobic interface. *Biochim. Biophys. Acta 643*, 191–204.
40. Subczynski, W. K., Wisniewska, A., Yin, J. J., Hyde, J. S., and Kusumi, A. (1994) Hydrophobic barriers of lipid bilayer membranes formed by reduction of water penetration by alkyl chain unsaturation and cholesterol. *Biochemistry 33*, 7670–7681.
41. Trodler, P., and Pleiss, J. (2008) Modeling structure and flexibility of *Candida antarctica* lipase B in organic solvents. *BMC Struct. Biol. 8*, 9.
42. Broos, J., Visser, A., Engbersen, J. F. J., Verboom, W., vanHoek, A., and Reinhoudt, D. N. (1995) Flexibility of enzymes suspended in organic solvents probed by time-resolved fluorescence anisotropy. Evidence that enzyme activity and enantioselectivity are directly related to enzyme flexibility. *J. Am. Chem. Soc. 117*, 12657–12663.
43. Aranganathan, S. (2005) Investigation of the Folding, Backbone Dynamics and Stability of The Antitumor Chromoprotein Neocarzinostatin. Ph.D. Thesis, National Tsing Hua University, Taiwan, Republic of China.
44. Zidek, L., Novotny, M. V., and Stone, M. J. (1999) Increased protein backbone conformational entropy upon hydrophobic ligand binding. *Nat. Struct. Biol. 6*, 1118–1121.
45. de Wolf, F. A., and Brett, G. M. (2000) Ligand-binding proteins: Their potential for application in systems for controlled delivery and uptake of ligands. *Pharmacol. Rev. 52*, 207–236.
46. Thorpe, I. F., and Brooks, C. L., III (2007) Molecular evolution of affinity and flexibility in the immune system. *Proc. Natl. Acad. Sci. U.S.A. 104*, 8821–8826.
47. Zavodszky, M. I., and Kuhn, L. A. (2005) Side-chain flexibility in protein-ligand binding: The minimal rotation hypothesis. *Protein Sci. 14*, 1104–1114.
48. Valente, A. P., Miyamoto, C. A., and Almeida, F. C. (2006) Implications of protein conformational diversity for binding and development of new biological active compounds. *Curr. Med. Chem. 13*, 3697–3703.
49. Lee, D., Damberger, F. F., Peng, G., Horst, R., Guntert, P., Nikonova, L., Leal, W. S., and Wuthrich, K. (2002) NMR structure of the unliganded *Bombyx mori* pheromone-binding protein at physiological pH. *FEBS Lett. 531*, 314–318.
50. Tarter, M., Capaldi, S., Carrizo, M. E., Ambrosi, E., Perduca, M., and Monaco, H. L. (2008) Crystal structure of human cellular retinol-binding protein II to 1.2 Å resolution. *Proteins 70*, 1626–1630.
51. Gillilan, R. E., Ayers, S. D., and Noy, N. (2007) Structural basis for activation of fatty acid-binding protein 4. *J. Mol. Biol. 372*, 1246–1260.
52. Torta, F., Dyuysekina, A. E., Cavazzini, D., Fantuzzi, A., Bychkova, V. E., and Rossi, G. L. (2004) Solvent-induced ligand dissociation and conformational states of cellular retinol-binding protein type I. *Biochim. Biophys. Acta 1703*, 21–29.
53. Povirk, L. F., Dattagupta, N., Warf, B. C., and Goldberg, I. H. (1981) Neocarzinostatin chromophore binds to deoxyribonucleic acid by intercalation. *Biochemistry 20*, 4007–4014.
54. White, S. H. (1976) The lipid bilayer as a "solvent" for small hydrophobic molecules. *Nature 262*, 421–422.
55. Wimley, W. C., and White, S. H. (1993) Membrane partitioning: Distinguishing bilayer effects from the hydrophobic effect. *Biochemistry 32*, 6307–6312.

56. Oda, T., and Maeda, H. (1987) Binding to and internalization by cultured cells of neocarzinostatin and enhancement of its actions by conjugation with lipophilic styrene-maleic acid copolymer. *Cancer Res. 47*, 3206–3211.
57. Schaus, S. E., Cavalieri, D., and Myers, A. G. (2001) Gene transcription analysis of *Saccharomyces cerevisiae* exposed to neocarzinostatin protein-chromophore complex reveals evidence of DNA damage, a potential mechanism of resistance, and consequences of prolonged exposure. *Proc. Natl. Acad. Sci. U.S.A. 98*, 11075–11080.
58. Shen, B., Liu, W., and Nonaka, K. (2003) Enediyne natural products: Biosynthesis and prospect towards engineering novel antitumor agents. *Curr. Med. Chem. 10*, 2317–2325.